16TH EUROPEAN CONFERENCE ON EARTHQUAKE ENGINEERING THESSALONIKI 18 - 21 JUNE 2018

ESTIMATION OF SHEAR-WAVE VELOCITY PROFILES BY JOINT INVERSION OF EARTHQUAKE GROUND MOTION DATA AND MICROTREMOR ARRAY DISPERSION DATA

Hiroyuki MIURA[1], Atsuko MATSUKO[2], Tatsuo KANNO[3], Michiko SHIGEFUJI[4], Tetsuo ABIRU[5]

ABSTRACT

A joint inversion technique using observed earthquake ground motion data and microtremor array dispersion data is developed to estimate the shear-wave velocity profiles at earthquake observation sites. Site amplification of shear-wave part in a seismic wave, receiver function extracted from earthquake ground motion data and phase velocity of surface wave extracted from microtremor array observation in Hofu City, Yamaguchi Prefecture, Japan are analyzed. Site amplifications are evaluated from Fourier spectral ratio between the soil site and the reference rock site. The shear-wave velocity profiles are estimated in the joint inversion by minimizing the total misfit between the observed and the theoretical data. We confirmed that the shear-wave velocity profiles inverted by the three features properly reproduce the observed site characteristics. In order to identify the two-dimensional subsurface structure in Hofu City, the inversion technique is applied to five seismic observation sites by assuming the unified shear-wave for deep underground model calibrated from the preliminary inversion analysis. The result shows that thickness of the sediment in the central part of the basin is larger than those in other sites, indicating the significant irregularity in the basin.

Keywords: Shear-Wave Velocity Profile; Site Amplification; Receiver Function; Phase Velocity; Joint Inversion

1. INTRODUCTION

In order to predict broad-band strong ground motion characteristics in a basin area, it is essential to identify the subsurface structure from ground surface to seismic bedrock (shear-wave velocity (Vs) = about 3km/s). Especially in the basin where an irregularly stratified structure is expected, estimating two- or three- dimensional change of the subsurface structure is important because strong local site amplification would be generated by the basin-induced focusing effect of the seismic waves. Recently an inversion technique of microtremor array dispersion data has been widely used to identify Vs profiles in a basin (Yamanaka et al. 1996, Okada 2003). Some researchers, however, pointed out that the site characteristics calculated from the microtremor dispersion-derived structure models sometimes do not match the observed ground motion characteristics because of the uncertainty of the observed dispersion data especially in long period range, and inversion of different kinds of observation simultaneously is an effective method to avoid the problem of non-uniqueness of inversion results (e.g., Kurose and Yamanaka 2006).

In this study, a joint inversion technique based on multiple ground motion characteristics is developed to identify shallow and deep Vs profiles using observed earthquake motion data and microtremor array dispersion data. We used site amplification with reference to the seismic bedrock and receiver function obtained from observed earthquake motion data, and phase velocity of Rayleigh wave extracted from microtremor array observation. The site amplifications and the receiver functions are sensitive to shallow soil profiles and deeper underground structures, respectively. These

[1]Associate Professor, Hiroshima University, Higashi-Hiroshima, Japan, hmiura@hiroshima-u.ac.jp
[2]The Chugoku Electric Power Company, Hiroshima, Japan, 767109@pnet.energia.co.jp
[3]Professor, Kyushu University, Fukuoka, Japan, kanno@arch.kyushu-u.ac.jp
[4]Assistant Professor, Kyushu University, Fukuoka, Japan, shigefuji@arch.kyushu-u.ac.jp
[5]General Manager, The Chugoku Electric Power Company, Hiroshima, Japan, 368753@pnet.energia.co.jp

characteristics reflect the P- and S- wave propagations. On the contrary, the phase velocity dispersions represents the characteristics of surface wave. The Vs profiles estimated from the joint inversion of these features are expected to satisfy the characteristics of the body wave and the surface wave in a basin, achieving more precise earthquake motion predictions for future earthquakes.

2. EARTHQUAKE GROUND MOTION AND MICROTREMOR ARRAY OBSERVATION

2.1 Target Area

We selected Hofu City, Yamaguchi Prefecture, Japan as the target area of this study. Hofu City is located on the Hofu basin, the largest basin area in the prefecture. The earthquake ground motions have been observed at K-NET (YMG013) and KiK-net (YMGH01) in the city as shown in Fig. 1. YMGH01 and YMG013 are located on the stiff and soft soil sites, respectively. According to the PS-logging investigation at YMGH01, the seismic bedrock with the Vs of 3km is found at the depth of 72m. The observed peak ground accelerations (PGA) at YMG013 are always several times larger than those at YMGH01, indicating that site conditions are dramatically changed between the sites.
In order to identify two-dimensional change of the underground structure in the basin, we have newly conducted the earthquake ground motion observations at four sites (KRN, SAB, HNG and NSU) since

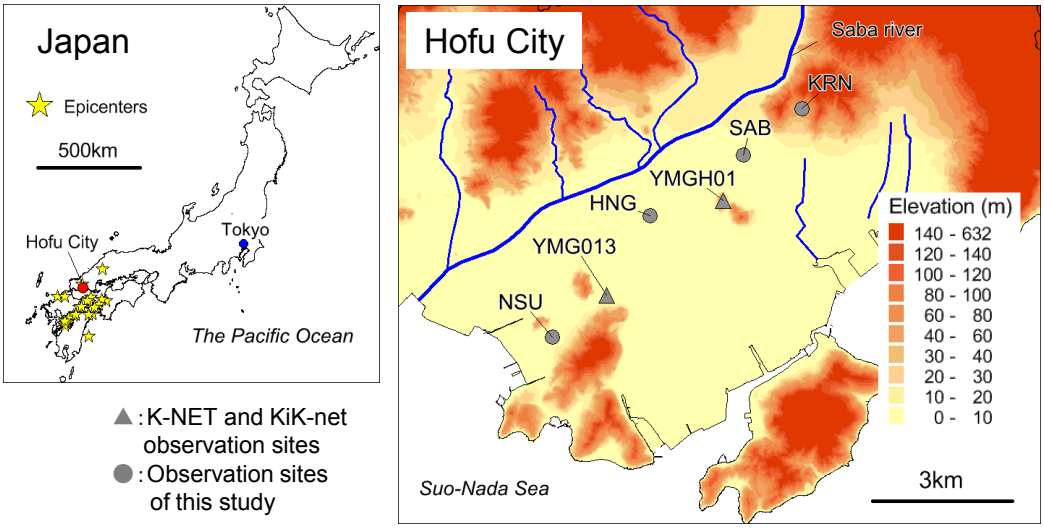

Fig. 1 Location of Hofu City, Japan with earthquake epicenters analyzed in this study (left). Distribution of earthquake observation sites in Hofu City, Yamaguchi Prefecture (right).

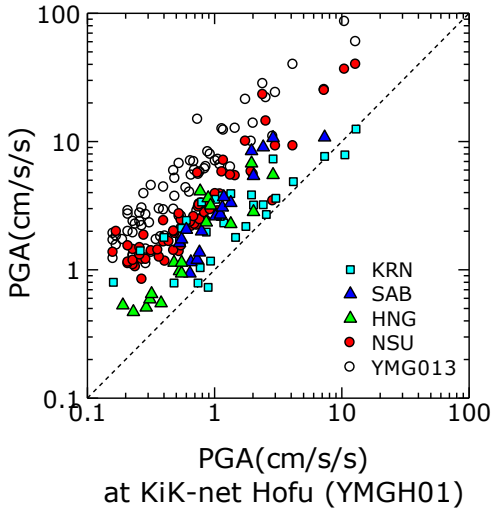

Fig. 2 Relationship of observed PGA between at YMGH01 and other sites

October 2014 to December 2016. The distribution of the observation sites is illustrated in Fig. 1. Totally 36 earthquakes have been recorded at the sites as shown in the left of Fig. 1. Figure 2 shows the relationship of observed PGA between YMGH01 and other sites. PGAs at the soil sites such as YMG013 and NSU are several to ten times larger than those at YMGH01.

2.2 Site Amplifications and Receiver Functions

The spectral site amplifications at YMG013 and YMGH01 at ground surface with reference to the seismic bedrock were already estimated by the spectral inversion of observed earthquake motion data (Kanno and Takeda 2012). In this study, the site amplifications at the newly installed observation sites are estimated from the spectral ratio with respect to YMGH01. Since the distances between the sites is much shorter than the hypocentral distances, the differences of the amplitudes by the geometric attenuation are not considered. The site amplification at the observation sites is calculated from the spectral ratio of the Fourier spectrum at the site divided by the spectrum at YMGH01, and multiplying the site amplification at YMGH01 to offset the amplification of YMGH01.
In order to examine the applicability of this method, the site amplification at YMGH03 is estimated from the spectral ratio as shown in Fig. 3. The spectral ratios with the frequency between 0.3 to 20Hz are analyzed. Figure 3(a) shows the spectral ratio of the earthquake motions between YMG013 and YMGH01, showing that the red line indicates the mean value of the spectral ratios. Figure 3(b) shows the comparison of the site amplifications estimated from the mean value of the spectral ratios and the site amplification obtained from the spectral inversion by Kanno and Takeda (2012), respectively. We confirm that the site amplification estimated from the spectral ratios shows good agreement with the result of the spectral inversion. The spectral ratio technique is applied to the records observed at other sites. Figure 4 shows the estimated site amplifications. While the fundamental frequency at KRN is approximately 7Hz, the frequencies at SAB and NSU are 2.5Hz. The predominant frequency at HNG is approximately 1Hz. These results suggest that the underground structure would be remarkably changed in the basin.
The receiver functions at each site are calculated from the deconvolution of the radial component and

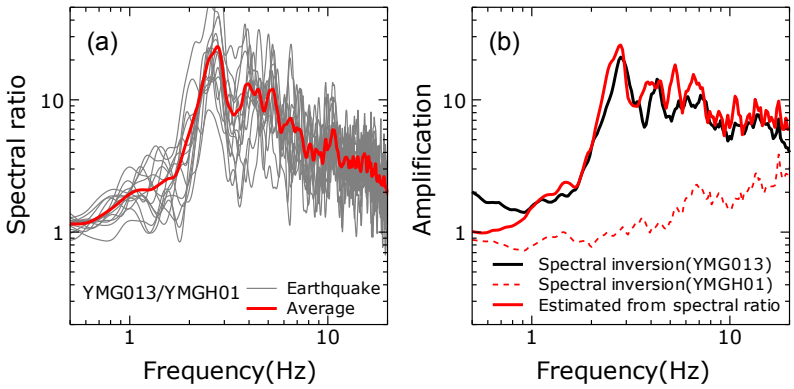

Fig. 3 (a) Fourier spectral ratio of YMG013 with reference to YMGH01, (b) Comparison of site amplification estimated in this study and obtained from spectral inversion technique (Kanno and Takeda 2012)

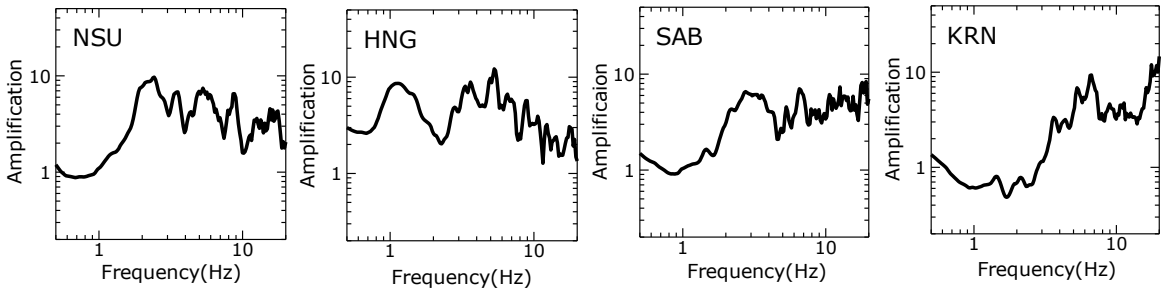

Fig. 4 Estimated site amplifications in observation sites

the vertical component of the observed records. The bandpass filter for the frequency between 1 to 10Hz is performed to the data. In order to reduce the effects of the Fourier amplitudes and emphasize the phase characteristics of the receiver functions, the amplitudes are set to 1 for all the data during the inverse Fourier transform. Figure 5 shows the calculated receiver functions at the sites. The mean values are shown by red lines. The timing of the peak in the receiver functions represents the arrival time difference between direct P-wave and PS converted wave (PS-P time) traveling in the sedimentary layers of the basin. In general, larger PS-P time indicates larger thickness of the deposits. The PS-P times at KRN, SAB, HNG, YMG013 and NSU are 0.03s, 0.12s, 0.30s, 0.14s and 0.14s, respectively. Smaller PS-P time at KRN and larger PS-P time at HNG suggest the thinner and thicker sediment, respectively that correspond to the trend of the site amplification as shown in Fig. 4.

2.3Rayleigh Wave Dispersion

The microtremor array observations are conducted at the sites to obtain the phase velocity of Rayleigh wave. The size of the arrays are shown in Table 1. Because of the limitation of the space at KRN, only miniature array observation with tie size of 0.6m is done. For the other sites, the array observations with the size of 1m to 40m are conducted. In order to identify the deep underground structure, larger array observation with the size of 500m at the maximum is performed at HNG. The CCA (Centerless Circular Array) method (Cho et al. 2004) is applied to the miniature array data and the SPAC (Spatial Autocorrelation) method (Aki 1957) is applied to the larger array data.
The estimated phase velocities of the fundamental mode Rayleigh waves are shown in Fig. 6. The phase velocities for only higher frequency than 20Hz are obtained at KRN. The result shows that the Vs of the surface ground at KRN is around 0.2km/s. The phase velocities of 1 to 2.5km/s at the maximum are estimated at other sites. The result at HNG indicates that the phase velocity dramatically increases at 2.5Hz or lower. The corner frequency determined by the rapid increase of the phase velocity is the lowest at HNG, indicating that largest thickness of the sedimentary deposits.

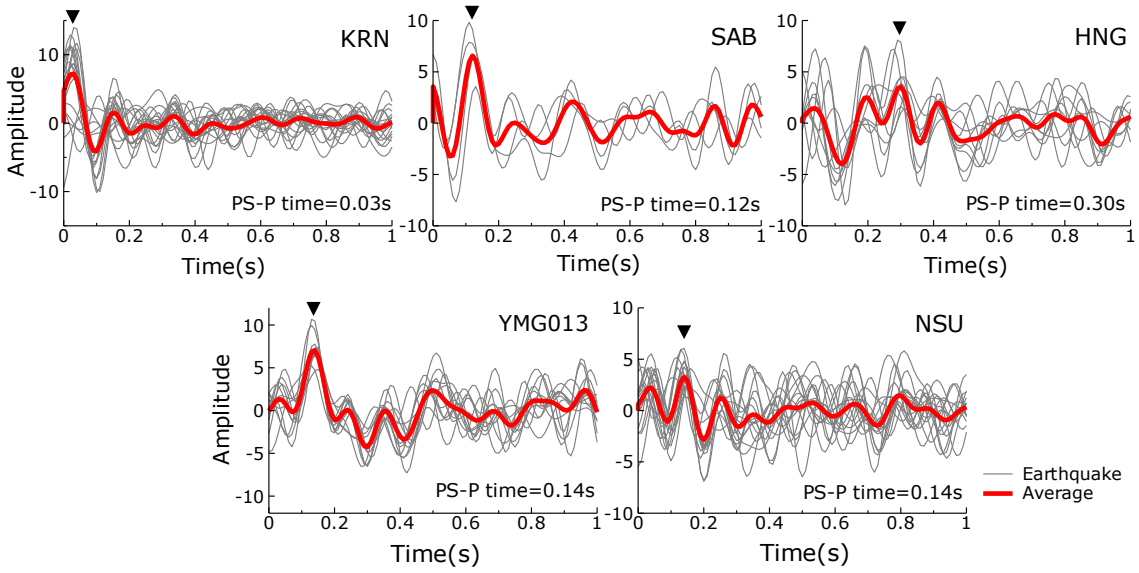

Fig. 5 Calculated receiver functions

Table 1 Conditions of microtremor array observations

Site	Array size in radius (m)	Observation date
KRN	0.6	Sep. 3, 2016
SAB	2, 5, 10, 20 and 40	Sep. 10, 2015
HNG	1, 2, 5, 10, 20, 40, 80, 270 and 500	Sep. 12, 2015 (1-40m), Sep. 3-4, 2016 (80-500m)
YMG013	2, 5, 12, 20, 30 and 40	Sep. 23, 2014 (2-12m), Sep. 14, 2015 (20-40m)
NSU	2, 5, 10, 20 and 40	Sep. 23, 2014

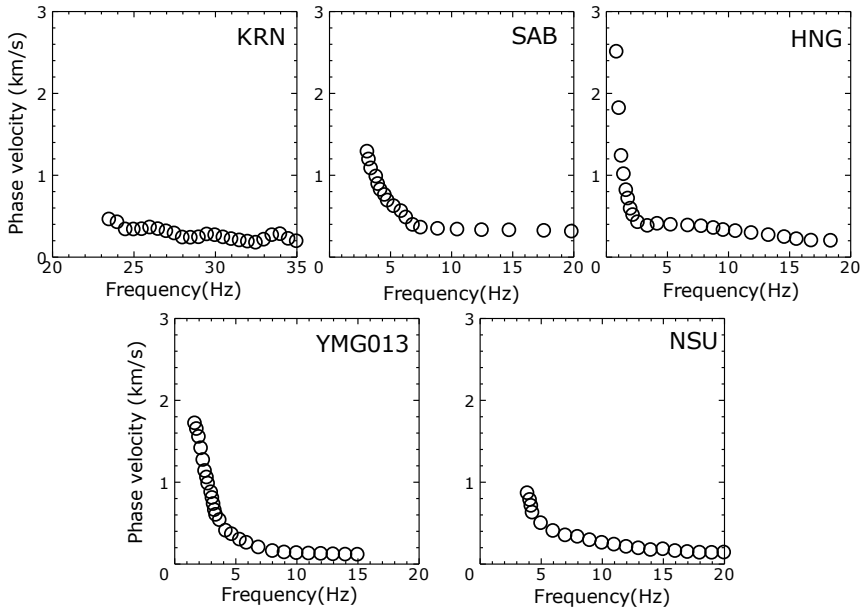

Fig. 6 Rayleigh wave phase velocities obtained from microtremor array observations

3. JOINT INVERSION TECHNIQUE

A joint inversion is applied to estimate the one-dimensional Vs profiles that can fit the observed site amplification, receiver function and Rayleigh wave phase velocity. A genetic algorithm (GA) is adopted in the joint inversion to find the best Vs profile by minimizing the misfit between the observed and theoretical data. The misfits of the data are calculated by the equations below.

$$misfit_A = \frac{1}{N_A}\sum_{i=1}^{N_A}\left(\frac{A_{obs}(f_i) - A_{cal}(f_i)}{A_{obs}(f_i)}\right)^2 \tag{1}$$

$$misfit_{RF} = \frac{1}{N_{RF}}\sum_{i=1}^{N_{RF}}\left(\frac{RF_{obs}(t_i) - RF_{cal}(t_i)}{RF_{obs}^{\max}(t_i)}\right)^2 \tag{2}$$

$$misfit_{PV} = \frac{1}{N_{PV}}\sum_{i=1}^{N_{PV}}\left(\frac{PV_{obs}(f_i) - PV_{cal}(f_i)}{PV_{obs}(f_i)}\right)^2 \tag{3}$$

$$misfit = p_A misfit_A + p_{RF} misfit_{RF} + p_{PV} misfit_{PV} \quad \text{where, } p_A + p_{RF} + p_{PV} = 1.0 \tag{4}$$

Here, $misfit_A$, $misfit_{RF}$, $misfit_{PV}$ and $misfit$ are indicate the misfits for site amplification, receiver function, phase velocity and their total, respectively. $A(f_i)$, $RF(t_i)$ and $PV(f_i)$ are the site amplification at frequency f_i, the receiver function at time t_i and the phase velocity at frequency f_i, respectively. The subscripts of *obs* and *cal* mean the observed and the theoretically calculated values from the model. N_A, N_{RF} and N_{PV} are the numbers of the data used in the inversion. The misfits are normalized by the numbers of the data because the dimensions and the number of the data are different from each other.

The factor p is a parameter ranging from 0 to 1, representing the weight of each data. When we preliminary assessed the joint inversion by using equal weights ($p_A = p_{RF} = p_{PV} = 0.333$), the theoretical values of the site amplification did not well match the observed data in some sites. Since

Table 2 Search areas of Vs and thickness for joint inversion

YMG013		
Layer	Vs(m/s)	H(m)
0	50-150	0-10
1	100-250	0-20
2	200-500	0-50
3	500-800	0-100
4	800-1800	0-200
5	1500-2700	0-200
6	3000	-

KRN, SAB, HNG, NSU		
Layer	Vs(m/s)	H(m)
1	100-250	0-20
2	200-500	0-50
3	500-800	0-100
4	800-1800	0-200
5	1500-2700	0-200
6	3000	-

the site amplification is important from the engineering point of view, the twice larger weight is given to the site amplification, indicating that $p_A = 0.5$ and $p_{RF} = p_{PV} = 0.25$ are used in the inversion. In the joint inversion, Vs and thickness of each layer are parameterized. P-wave velocity and densities are calculated during the inversion by the empirical relationship by Kitsunezaki et al. (1991) and Dal Moro et al. (2007), respectively.

Two-step inversion approach is adopted in order to identify the two-demensional change of the thickness of deep soil deposits. In the first step, search areas for the Vs and thickness of each layer are set as shown in Table 2. Since very soft soil layer is expected at the ground surface of YMG013 from the result of the Rayleigh wave phase velocity, seven layers are set in the inversion. Six layers are assumed at other sites. In the second step, mean values of the Vs for the layers deeper than the third layer among the sites are calculated from the results of the first step. The mean values of the Vs are fixed and only the thicknesses are parameterized for the deeper layers in the second step inversion.

4. ESTIMATION OF VS PROFILES

Figure 7 shows the results of the joint inversion at the five observation sites in Hofu City. Black lines in the site amplifications, receiver functions and the phase velocities indicate the observed data. Blue lines represent the theoretical data from the first step inversions. Right side of the figures indicate the inverted Vs profiles. In order to compare with the existing subsurface structure models in J-SHIS (NIED 2017), the Vs profiles in the J-SHIS model are illustrated by black lines. We confirm that the theoretical values obtained from the first step inversion shows good agreement with the observed data. Figure 8 shows the distribution of the inverted Vs for the deep layers. Red circles represent the mean values of the inverted Vs. The second step inversion are applied by using the mean values of the Vs for the deep layers.

Red lines in Fig. 7 show the results of the second step inversions. The theoretical data by the second inversion almost match not only the results by the first inversion but also the observed data. Figure 9 shows the distribution of the thickness for the deep layers obtained during the second inversions. The values indicate the results for best five cases that smallest misfit are obtained in the inversions. Red circles mean the best results adopted in this study. Since the variances of the thickness are quite small, the thicknesses are converged to the unique values in the joint inversion.

In order to validate the proposing joint inversion, the estimated Vs profiles need to be compared to other geophysical exploration data. In this area, however, information for deep underground structure is not available other than the J-SHIS model. Then NIED has already estimated the Vs profiles in the J-SHIS model at strong motion observation sites including YMG013 by using the ground motion observation records. This means that more accurate Vs profiles are obtained at the existing observation sites in the J-SHIS model. The Vs profile at YMG013 estimated in this study shows good agreement with the J-SHIS model, indirectly indicating the validity of the joint inversion technique.

The basement depths to the seismic bedrock are about 50m at KRN, 150 to 200m at SAB, 350 to 400m at HNG, 150 to 200m at YMG013 and 100 to 150m at NSU, respectively. The depth at HNG is remarkably larger than the depths at other site and the existing J-SHIS model. Figure 10 shows the cross section of the estimated Vs profiles along the observation line (northeast-southwest) in the basin.

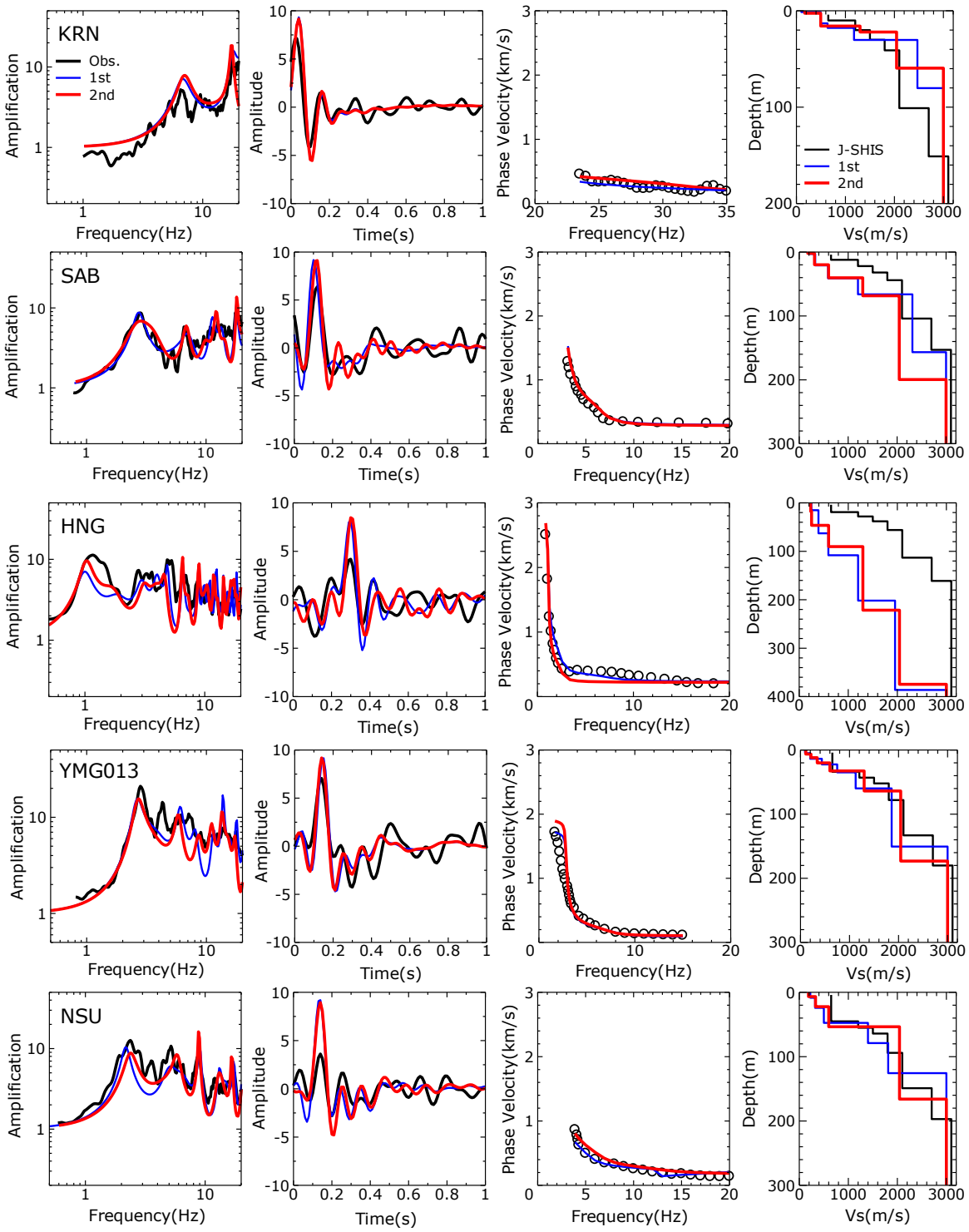

Fig. 7 Results of joint inversions and estimated Vs profiles

The upper bounds of the seismic bedrock in the J-SHIS model are also illustrated by the dotted lines. The basement depth at KRN located in the hilly area is smaller than that in the J-SHIS model. The basement depth at SAB, YMG013 and NSU almost agree with those in the J-SHIS model. On the contrary, the basement depth at HNG is much larger than that in the J-SHIS model. These results suggest that the irregularly stratified soil structure is expected in the center of the basin, and the 3D underground structure would be more complex than the existing model.

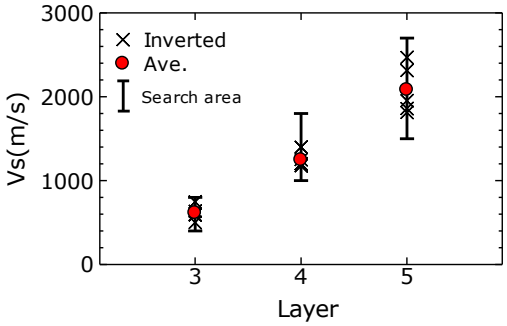

Fig. 8 Distribution of estimated Vs for deep layers in the first step inversion

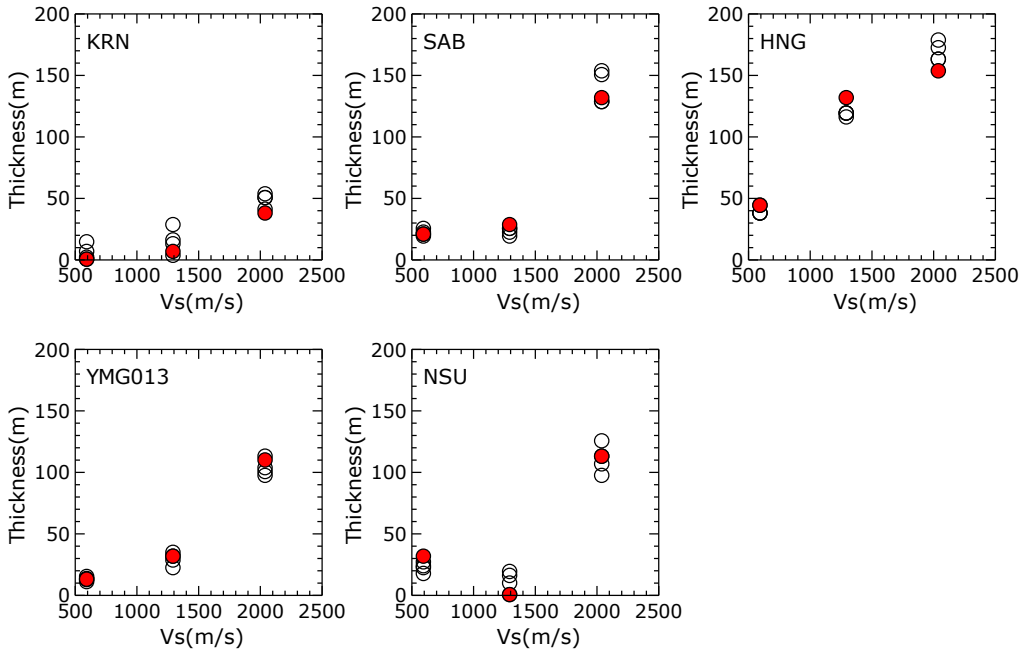

Fig. 9 Distribution of estimated thickness for deep layers in each site during the second step inversion

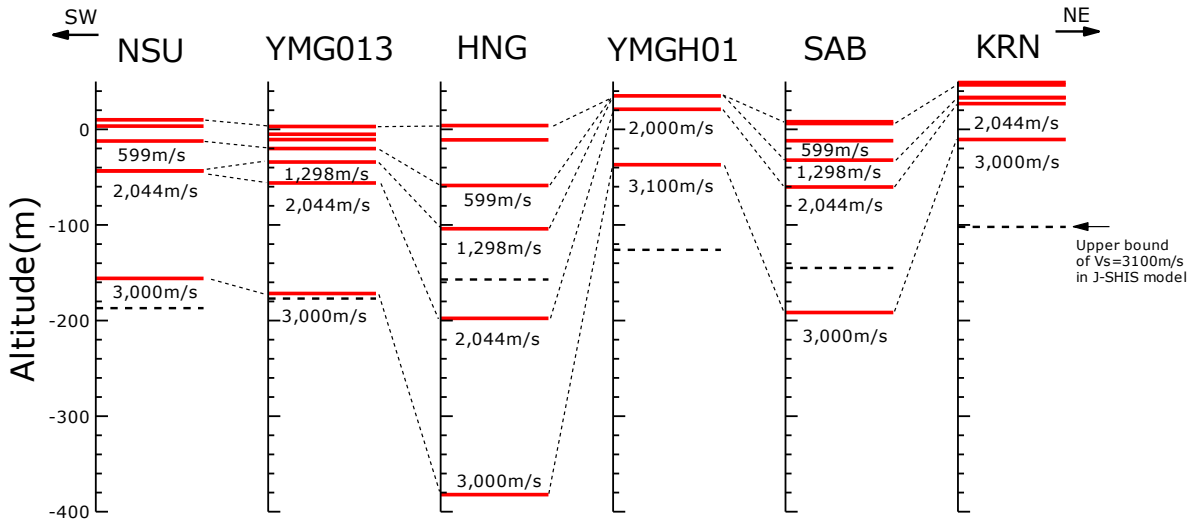

Fig. 10 Cross section of Vs profiles along observation line in the Hofu basin

5. CONCLUSIONS

This paper introduced a joint inversion technique to identify the Vs profile from surface ground to the seismic bedrock by using the earthquake observation records and Rayleigh wave phase velocities obtained from microtemor array observation. The method was applied to the observation data in Hofu City, Yamaguchi Prefecture, Japan. Site amplifications were estimated from the spectral ratio of the earthquake motion data with reference to the spectrum observed at YMGH01 where rock is exposed nearly on the surface. We confirmed that the estimated site amplification shows good agreement with that obtained from the spectral inversion technique. Receiver functions were calculated from the deconvolution of the radial component to vertical component of the earthquake motion data. Rayleigh wave phase velocities were extracted by the CCA method for miniature array data and the SPAC method for other array data. The joint inversion method based on the three ground motion characteristics were developed. We confirmed that the estimated Vs profile models well reproduced the observed data. The results of the inversions revealed the significant irregularly stratified soil structure in the central part of the Hofu basin.

6. ACKNOWLEDGMENTS

The authors acknowledge the member of Disaster Prevention Engineering laboratory in Hiroshima University and Urban Environment Risk Systems laboratory in Kyushu University for helping the microtremor array observations.

7. REFERENCES

Aki K (1957). Space and time spectra of stationary stochastic waves, with special reference to microtremors, *Bull. Earthq. Res. Inst.*, 35: 415-456.

Cho I, Tada T, Shinozaki Y (2004). A new method to determine phase velocities of Rayleigh waves from microseisms. *Geophysics* 69(6): 1535-1551.

Dal Moro G, Pipan M. Gabrielli P (2007) Rayleigh wave dispersion curve inversion via genetic algorithms and marginal posterior probability density estimation. *Journal of Applied Geophysics* 61: 39-55.

Kanno T, Takeda J (2012). Study on constraint condition for spectral inversion technique. *Proceedings of 15th World Conference on Earthquake Engineering*, Paper No.2816, September, Lisbon, Portugal.

Kitsunezaki C et al. (1990). Estimation of P- and S-wave velocities in deep soil deposits for evaluating ground vibrations in earthquake. *Journal of the Japan Society for Natural Disaster Science* 9: 1-17 (in Japanese with English abstract).

Kurose T, Yamanaka H (2006). Joint inversion of receiver function and surface-wave phase velocity for estimation of shear-wave velocity of sedimentary layers. *Exploration Geophysics* 37: 93-101.

National Research Institute for Earth Science and Disaster Resilience (NIED) (2017). Japan Seismic Hazard Information Station (J-SHIS). http://www.j-shis.bosai.go.jp/en/ (accessed in August 2017 and the Subsurface Structure V2 model was updated in 2012).

Okada H (2003). *The microtremor survey method*. Geophysical Monograph Series No. 12, Society of Exploration Geophysics.

Yamanaka H, Ishida H (1996). Application of genetic algorithms to an inversion of surface-wave dispersion data, *Bull. Seism. Soc. Am.*, 86(2): 436-444.